Positronium in a SrF_2 single crystal: Temperature-induced transition from the localized to the delocalized state

K. Inoue,[1,*] N. Suzuki,[2,†] and T. Hyodo[1]
[1]*Institute of Physics, Graduate School of Arts and Sciences, University of Tokyo, 3-8-1 Komaba, Meguro-ku, Tokyo 153-8902, Japan*
[2]*The Institute of Physical and Chemical Research(RIKEN), Hirosawa, Wako-shi, Saitama 351-0198, Japan*
(Received 5 February 2005; published 22 April 2005)

Formation of positronium (Ps) in SrF_2 single crystal is confirmed. Temperature dependence of the momentum distribution and the lifetime of the Ps have been investigated in the temperature range from 10 to 297 K. Temperature induced transition of the Ps from the localized to the delocalized state has been observed. At low temperatures, the Ps is in the localized state. When the temperature is above about 100 K, the Ps in the localized states coexists with that in the delocalized states. The intensity of the delocalized Ps component increases as the temperature rises. The effective mass of the delocalized Ps is found to be $6.3\times 2m$, considerably larger than the free Ps mass ($2m$) in vacuum. The level of the bottom of the delocalized state is 0.012 eV higher than that of the localized state.

DOI: 10.1103/PhysRevB.71.134305 PACS number(s): 71.35.−y, 36.10.Dr, 78.70.Bj

I. INTRODUCTION

Positronium (Ps), which is the bound state of a positron and an electron, forms in various insulating solids, e.g., alkali halides, SiO_2, polymers, etc.[1–4] The Ps in solids can be said to be an isotope of the exciton, a bound state of an electron and a hole.

While Ps in crystalline SiO_2 is in a delocalized Bloch state,[5] Ps in alkali halides (NaF, NaCl, NaI, KCl, KBr, and KI) exists in two kinds of states, delocalized and localized (self-trapped) states. The energy level of the localized state is a little higher than the bottom of the delocalized band, i.e., the localized state is metastable.[1,2,6–12] At low temperatures (typically less than a few tens of K), the Ps populates mainly the delocalized states. This is confirmed by the observation of very narrow peaks in the momentum distribution of the positron annihilation radiation, the central peak and the satellite peaks appearing at the momenta corresponding to the reciprocal lattice vectors of the specimen crystal. As the temperature rises, Ps tends to be self-trapped, resulting in a marked broadening in its center-of-mass momentum distribution. Similar coexistence of the free and the self-trapped components has been observed in the exciton luminescence spectra of several materials.[13–15] Since the band mass of the positron in alkali halides is smaller than that of the hole,[16] the Ps in the same materials has a smaller mass than the exciton. Hence the Ps is more difficult to be localized and it has some influence on that the self-trapped state of Ps in the above mentioned alkali halides is metastable.

Excitons in alkaline earth fluorides has been investigated and well understood,[14,17,18] however Ps in these materials, except for MgF_2,[19,20] has not been studied even in relation to its formation. In the present work, we investigate the existence and the behavior of Ps in SrF_2. In the next section, the experimental methods used are described. Experimental results are shown and analyzed in the third section and a discussion of the results is presented in the fourth section. Finally a summary is given in the last section.

II. EXPERIMENTAL PROCEDURE

High resolution one-dimensional angular correlation of positron annihilation radiation (1D-ACAR) measurements and positron lifetime measurements have been performed on SrF_2.

SrF_2 single crystals used in both the 1D-ACAR and the positron lifetime experiments were supplied by OKEN Co. Ltd. In the 1D-ACAR measurements, the specimen was glued onto a copper plate with GE 7031 varnish, and mounted on the cold finger of a closed-cycle helium refrigerator fitted to a vacuum-tight chamber such that the $\langle 100\rangle$ axis of the crystal was oriented parallel to the measured momentum direction. To avoid asymmetric absorption of the annihilation γ rays in the sample, the top surface of the specimen was cut at an angle of about 3° to the (100) plane of the crystal. The surface of the specimen was coated with vacuum-evaporated aluminum to avoid charge pileup during the measurements. Positron annihilations in the thin aluminum coating were estimated to be negligible. The specimen temperature was controlled to within ±0.5 K at values below room temperature. Measurements were also performed at room temperature, 297±1 K. A positron source of 30 mCi of ^{22}Na was placed outside the vacuum chamber, facing the specimen across a 40 μm thick beryllium window.

The 1D projection of the electron-positron momentum distribution onto the $\langle 100\rangle$ direction of the crystal was measured in a magnetic field of +1.1 T. The positive (negative) sign indicates the direction of the field parallel (antiparallel) to the positron incident direction. The momentum resolution was $0.45\times 10^{-3}mc$ (m is the free electron mass, c is the speed of light, $mc=137$ a.u.) full width at half maximum (FWHM). In order to confirm unambiguously that Ps was formed, momentum distribution was also measured in a magnetic field of −1.1 T at several temperatures. Confirmation of the Ps formation by this method is based on the fact that the positrons emitted from a β^+ decay source are spin-polarized along their momenta. The 2γ self-annihilation of the Ps is more enhanced when the magnetic field is parallel to the

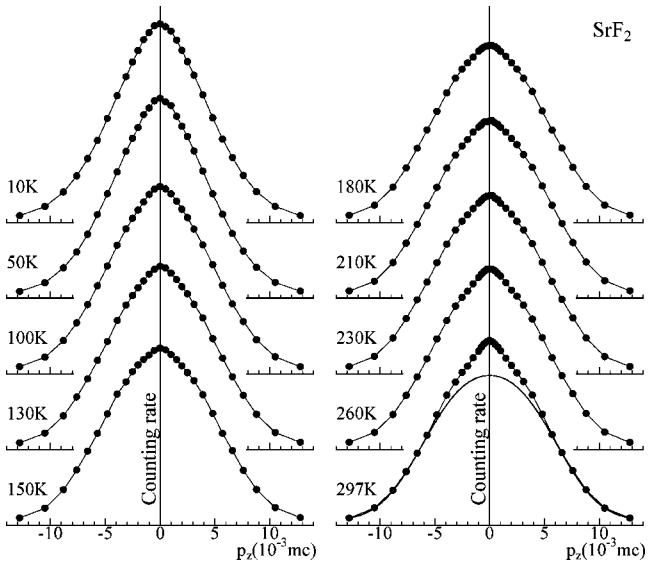

FIG. 1. Momentum distributions of the annihilation photons along the ⟨100⟩ axis of SrF_2 in the temperature range 10–297 K.

positron spin than in the opposite case.[11] Comparing the data for the magnetic fields of the same intensity but with opposite polarities diminishes possible errors induced by the difference in the area sampled by the positrons.

The positron lifetime was measured in the temperature range from 10 K to room temperature. The positron source used for the lifetime measurements was ^{22}Na of approximately 10 μCi deposited onto Kapton foil which was then covered with another piece of foil. The source was sandwiched between two identical pieces of the crystal specimen. A pair of fast scintillation counters were used to provide the signals required to measure the positron lifetime. One of the detectors was used to detect the 1.275 MeV nuclear γ rays from the β^+ decay of ^{22}Na, giving the start signals, whilst the stop signals were provided by the 511 keV annihilation γ rays detected at the other counter. The time resolution was 220 ps (FWHM).

III. EXPERIMENTAL RESULTS

The momentum distributions obtained at various temperatures from the 1D-ACAR experiment are shown in Fig. 1, where the 2γ coincidence counting rate is plotted against momentum, p_z.

The data was found to be temperature dependent; a cusp-like structure was found at the center of the momentum distributions at temperatures near room temperature. Such a structure was not observed at low temperatures.

Figure 2 shows the result of the subtraction of the momentum distributions in the magnetic field −1.1 T from those taken in +1.1 T after appropriate normalization. (The normalization was performed in the following way.[11] The ratio of the two curves was plotted against momentum; it was found that this ratio was almost constant for $|p_z| > 7 \times 10^{-3} mc$. This indicates that the change in the field polarization does not appreciably alter the shape of the broad component. Then the two curves were normalized to the areas in the regions $|p_z| > 7 \times 10^{-3} mc$.) The existence of the remaining component is definite evidence for the existence of Ps in SrF_2, the component giving the momentum distribution of the Ps. The momentum distribution of the Ps at 10 K thus obtained was approximated by a single Gaussian function of width $6.0 \times 10^{-3} mc$ at FWHM. The Ps momentum distribution at values near room temperature contains two components where the width of one of these components is very narrow. This gives rise to the cusp seen in the raw data, shown in Fig. 1.

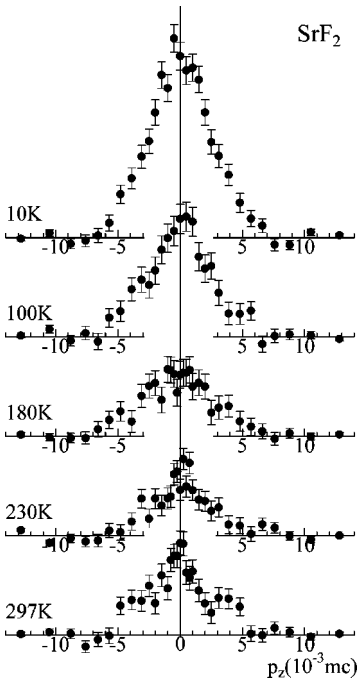

FIG. 2. Positronium momentum distribution in SrF_2 obtained using the effect of the spin-polarization on Ps formation.

In order to investigate the temperature dependence of the Ps components with better statistics, we subtracted from every curve the broad component which resulted from the annihilation of the positrons with electrons of the SrF_2 or the pick-off annihilation of the Ps. The shape of the momentum distribution, $F(p_z)$, was represented as

$$F(p_z) = F_1(p_z) + F_2(p_z) + F_3(p_z), \tag{1}$$

where

$$F_1(p_z) = a \exp(-\alpha p_z^2),$$

$$F_2(p_z) = b \exp(-\beta p_z^2),$$

$$F_3(p_z) = c(\exp(-\eta p_z^2) + d \exp[-\xi(p_z - g)^2] + d \exp[-\xi(p_z + g)^2]).$$

The parameters were determined by simultaneously fitting

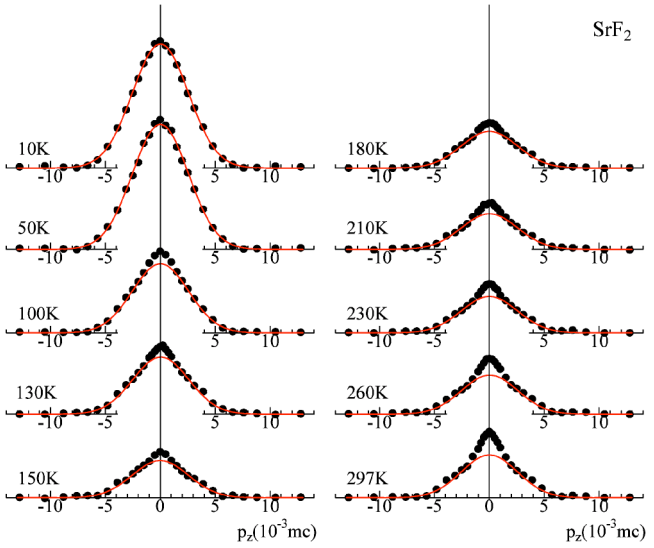

FIG. 3. (Color online) The temperature dependence of the Ps momentum distribution in SrF_2 obtained by subtracting the broad component from the momentum distribution in Fig. 1. The solid line indicates the component of Ps in the localized state.

the function (1) to the six ACAR data results at 180 K, 230 K, and 297 K for the magnetic fields +1.1 T and −1.1 T. The function, $F_1(p_z)$, represents the narrow Ps component, $F_2(p_z)$ represents the broader Ps component, and $F_3(p_z)$ represents the common broad component showing the momentum distribution of the γ rays from positron annihilation with the electrons of the SrF_2. A more complex function for $F_3(p_z)$ was introduced after finding that using a single Gaussian was not adequate. A constraint of the fitting was that β was fixed to give a width of $6.0\times10^{-3}mc$, as determined in the magnetic quenching experiments and η, ξ, d, and g were parameters common to all six ACAR curves. The parameter α was common to the data for the same temperature with both the magnetic fields used (+1.1 T and −1.1 T) but dependent on the temperature. The Ps component which is isolated by subtracting the obtained common broad component, $F_3(p_z)$, (shown in Fig. 1 on the 297 K plot) from each of the momentum distributions is shown in Fig. 3 together with the fitted $F_2(p_z)$.

The results of the two-component analysis of the lifetime spectra are shown in Fig. 4. The intensity of the long lifetime component, I_2, decreases as the temperature rises and starts to increase at around 180 K. The long lifetime, τ_2, starts to shorten gradually at around 100 K. The short lifetime, τ_1, becomes longer as the temperature rises to 180 K and appears to be almost constant or even slightly decreases as the temperature rises above 180 K.

IV. DISCUSSION

The temperature dependence of the momentum distribution $F_1(p_z)+F_2(p_z)$ (shown in Fig. 3) corresponds to the temperature dependence of the population of Ps in the two different states, which is in agreement with that obtained by magnetic effect (shown in Fig. 2). There is no theoretical

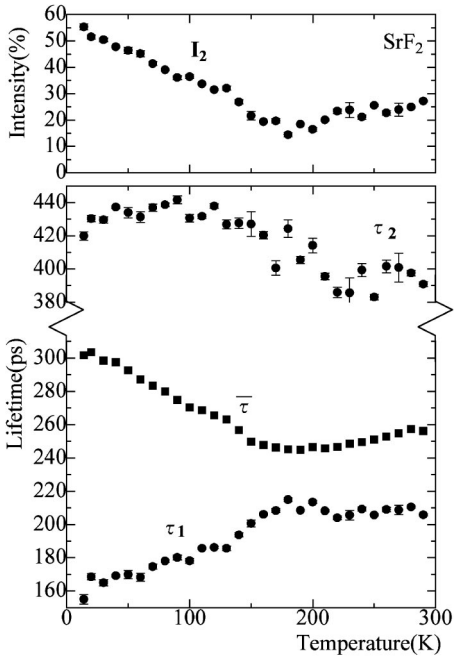

FIG. 4. The short lifetime, τ_1, the long lifetime, τ_2, the average lifetime, $\overline{\tau}$, and the intensity of the long lifetime component, I_2, of the positron lifetime in SrF_2.

calculation available of the broad component, $F_3(p_z)$, resulting from the annihilation of the non-Ps positrons and the pick-off annihilation of the Ps in SrF_2. In the following, we shall make no further discussion on this component.

Figure 5 shows the momentum distribution around the momentum corresponding to the projection of the first reciprocal lattice vector $(4.2\times10^{-3}mc)$ measured at 297 K with high statistics. A small structure is seen indicating a higher momentum component of the narrow Ps component. To make this point clear, Fig. 6 shows the component obtained by subtracting the fitted function, $F_2(p_z)$ and $F_3(p_z)$, from the ACAR data at 297 K. A main peak at zero momentum and

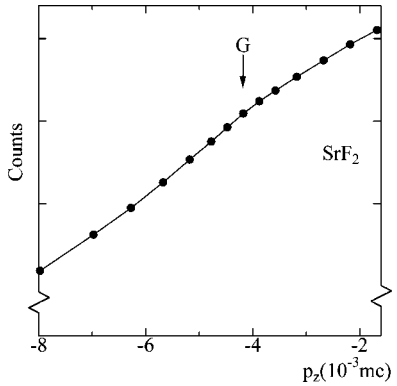

FIG. 5. Momentum distribution around the momentum corresponding to the reciprocal lattice vector of SrF_2. The arrow pointing in the figure represents the momentum corresponding to the reciprocal lattice vector of SrF_2.

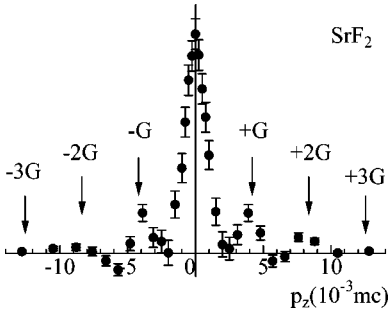

FIG. 6. Momentum distribution of delocalized Ps at 297 K in SrF_2. G represents the reciprocal lattice vector of SrF_2.

satellite peaks at around multiples of the reciprocal lattice vectors $\pm 4 \times 10^{-3} mc$ are clearly visible. Figure 7 shows the temperature dependence of the square of the width (FWHM) of the central narrow component, W_1. In the temperature region above 150 K, the square of the width increases linearly with temperature. These show that the narrow component results from the self-annihilation of the Ps in the delocalized (Bloch) state with energy-momentum relation characterized by a constant effective mass. If we assume that the momentum distribution of these Ps atoms, $F_1(p_z)$, is described by the Boltzmann distribution with an effective mass M^*,

$$F_1(p_z) \propto \exp(-p_z^2/2M^* k_B T), \tag{2}$$

then the width (FWHM) of the narrow component, W_1, is expected to vary with temperature as

$$W_1 = [8(\log 2) M^* k_B T]^{1/2}. \tag{3}$$

The experimental value for M^* is derived from the slope of the W_1^2 vs T plot, shown in Fig. 7. The solid line in the figure shows the result of the least-squares fit to the data. From the slope of this line, we conclude that the effective mass, M^*, of delocalized Ps in SrF_2 is $(6.3 \pm 0.2) \times 2m$. This value is

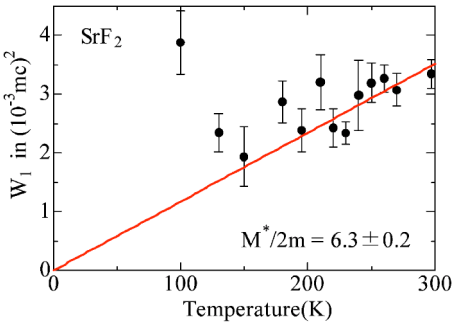

FIG. 7. (Color online) Temperature dependence of the square of the width (FWHM) of the narrow component of the Ps peak in SrF_2. The width has been corrected for the broadening due to the optical resolution of the apparatus. The solid line shows the result of the least-squares fit to the data, from the slope of which the effective mass, M^*, of the Bloch Ps in SrF_2 is found to be $(6.3 \pm 0.2) \times 2m$.

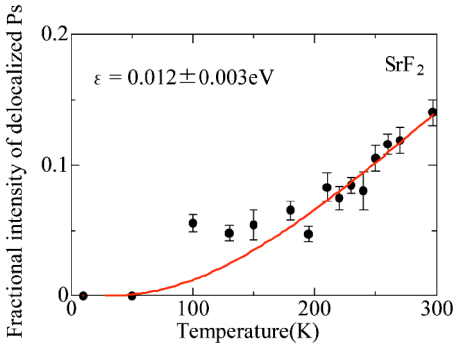

FIG. 8. (Color online) Temperature dependence of the fractional intensity of the delocalized Ps in SrF_2. The full circles show the experimental data derived from the Ps peaks shown in Fig. 3, while the solid line represents the least-squares fitted theoretical curve which corresponds to the level of the delocalized state $\varepsilon = 0.012$ eV.

considerably larger than those of delocalized Ps in alkali halides. At temperatures below 130 K, the experimental data points lie above the fitted line. This is perhaps because the Ps in this temperature range is in an intermediate state between a free and a localized state, somewhat like a loaded free state.[21] The Ps in this state is free to move but only slowly with a heavy load of the phonon cloud.

The broader Ps component, $F_2(p_z)$, is due to the self-annihilation of the Ps in the localized state. The width of the momentum distribution of the localized Ps is independent of temperature.

The temperature dependence of the Ps components (shown in Fig. 3) indicates that the Ps is localized at temperatures lower than about 100 K and the transition from the localized to the delocalized states takes place when the temperatures rises above about 100 K. The fractional intensity of the delocalized Ps component, $S_1/(S_1+S_2)$, is plotted against temperature in Fig. 8, where S_1 and S_2 are the intensities of the delocalized and the localized Ps components, respectively.

Temperature dependence of the delocalized Ps intensities in SrF_2 displays contrast to that of the Ps in alkali halides.[8] In alkali halides the Ps populates mainly the delocalized states at temperatures lower than a few tens of K. As the temperature rises, it tends to be self-trapped. At values near room temperature, all the Ps atoms are self-trapped. A model proposed to interpret metastable self-trapping of holes in some metal halides[22] has been applied by Hyodo *et al.*[7] to explain the temperature dependence of the momentum distribution of Ps in alkali halides. This model assumes that the level of the self-trapped state is situated lower (by ε) than the bottom of the delocalized Ps band, and the fraction of the Ps in the delocalized state, f_F, is given by

$$f_F = 1/[1 + AT^{-3/2} \exp(\varepsilon/k_B T)], \tag{4}$$

where $A = N/V(2\pi\hbar^2/M^* k_B)^{3/2}$, V, is the volume of the crystal, and N is the number of the possible localized sites for the

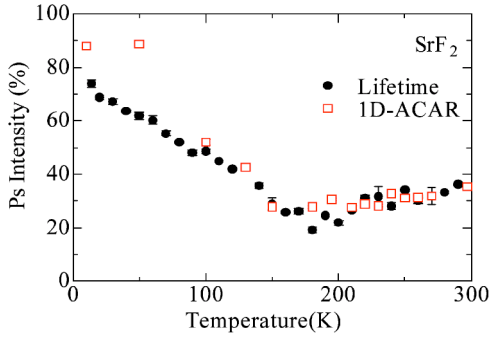

FIG. 9. (Color online) Comparison of Ps intensities obtained from lifetime measurements (closed circles) and ACAR measurements (open squares).

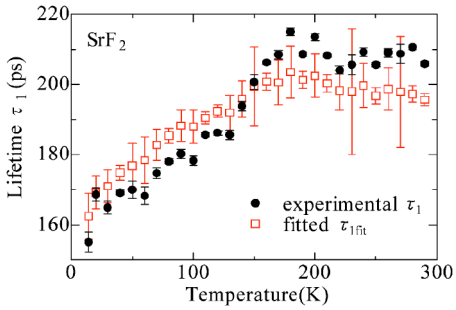

FIG. 10. (Color online) Comparison of the experimentally obtained short lifetime (closed circles) and the fitted lifetime (open squares) from the intensity of the long lifetime component.

Ps in the crystal. For Ps in alkali halides, ε is negative; the self-trapped state of Ps is metastable.

This model can be applied without any modification to the case of the Ps in SrF_2. The fraction, f_F, given by Eq. (4) was fitted to the fractional intensity of the narrow component, shown in Fig. 8. The solid line in the figure shows f_F fitted to the data with ε and N being adjustable parameters and with the constraint that $M^* = 6.3 \times 2m$. The general feature of the observed temperature dependence of the momentum distribution has been reproduced reasonably well. The fitting gives the value of ε as (0.012 ± 0.003) eV and the number of localized sites per unit cell, N, as (0.4 ± 0.1). When the specimen temperature rises, the effective number of the available delocalized states increases rapidly because of the large effective mass of the Ps.

Turning to the results of the positron lifetime measurements, shown in Fig. 4, these can be interpreted in the light of the results from the ACAR experiments. The lifetime spectra consist of the annihilation of two Ps components, para-Ps (p-Ps) and ortho-Ps (o-Ps), and that of the non-Ps positrons (free positrons). In an insulating single crystal in which Ps exists, the short lifetime, τ_1, component in a two component analysis contains the annihilation of p-Ps and free positrons, which cannot be resolved with the time resolution of the present apparatus. The long lifetime, τ_2, component is due to o-Ps as the lifetime of the o-Ps is usually much longer than that of the p-Ps and the free positrons.[3]

The closed circles and the open squares in Fig. 9 represent the temperature dependence of the total Ps intensity estimated from the lifetime data and ACAR data, respectively. The total Ps intensity from the lifetime data is estimated by multiplying o-Ps intensity by 4/3, due to the statistical weighting of the para and ortho spin states. The total Ps intensity from the ACAR data is calculated from the intensity of the Ps peak as follows. The Ps peak arises from the self-annihilation of the Ps. We took pick-off annihilation into account. We also took the magnetic quenching effect into account since the ACAR measurements were performed under the magnetic field. The applied magnetic field mixes the p-Ps state with the $m_s = 0$ substate of the o-Ps,[10] which causes 2γ self-annihilation of the perturbed o-Ps. Moreover, the ratio of the p-Ps and the o-Ps intensities changes from 1/3 depending on the magnetic field because the positrons incident onto the sample from the source are spin-polarized along the field direction. We used the theoretical 2γ annihilation intensities of Ps as a function of magnetic field.[23,24] The polarization of the positrons along the magnetic field was 0.3, as measured by the present apparatus,[24] and the pick-off annihilation rate was $1/400$ ps^{-1} estimated from the lifetime τ_2. The self-annihilation rate in SrF_2 is not necessarily the same as that in vacuum because of the screening of the Coulomb interaction of the constituent particles of Ps by the electrons of the medium. This makes the average distance of the electron and the positron in Ps larger and the contact density of these particles smaller. Hence the self-annihilation rate of Ps decreases. The contact of the positron with the medium electrons, on the other hand, causes pick-off annihilation. In this experiment, detailed information on the self-annihilation rate of p-Ps in SrF_2 could not be obtained. As a rough approximation, we presumed the overall annihilation rate of p-Ps is the same as the self-annihilation rate in vacuum ($1/125$ ps^{-1}). We see in Fig. 9, that the Ps intensities estimated are in good agreement with that estimated from the ACAR experiment.

Correlation between the short lifetime, τ_1, and the intensity of the o-Ps, I_2, can be explained if we assume that the lifetime of the p-Ps is shorter than that of the free positrons as is usually the case with Ps in solids. Figure 10 shows the temperature dependence of the short lifetime, τ_{1fit}, fitted by setting the free positron lifetime using a free parameter which is independent of temperature. The lifetime which gives the best fit is 210 ps, close to the value of the free positron lifetime in alkali halides reported previously.[9]

The almost constant lifetime of the o-Ps, τ_2, below 100 K is consistent with the indication from the ACAR data that all the Ps atoms are in the localized state below 100 K. If we assume that the localization of the Ps is accompanied by a local dilation of the lattice, as in alkali halides,[9,10] the decrease of the long lifetime, τ_2, becoming shorter above 100 K is consistent with the fractional increase of delocalized Ps, as suggested by the ACAR measurements. The increase in the fraction of the Ps delocalized in a region with low electron density makes the average o-Ps lifetime shorter.[9]

The localized state is the intrinsic self-trapped state, judging from the fitted number of localized states per unit cell in the present model. If the localized state is attributed to

impurity induced extrinsic self-trapped state,[13] the fitted number of localized state must be much smaller than the observed value.

V. SUMMARY

We have investigated positron annihilation in SrF_2 single crystal. Formation of Ps is confirmed. Temperature induced transition of the Ps from the localized to the delocalized state has been observed in both the momentum distribution and the lifetime measurements. The effective mass of the delocalized Ps is determined to be 6.3 ± 0.2 in units of $2m$. The level of the localized state is found to be 0.012 ± 0.003 eV lower than the delocalized state.

ACKNOWLEDGMENTS

The authors express thanks to Dr. H. Saito for his support during the experiments and also thanks to Professor Y. Kubo and Dr. A. Kodama for the results of the theoretical electron momentum distribution and to Dr. Z. Tang for valuable discussions.

*Present address: The Oarai branch, Institute for Materials Research, Tohoku University, Oarai City, Higashi-ibaraki-gun, Ibaraki 311-1313, Japan. Electronic address: kinoue@imr.tohoku.ac.jp

†Present address: Molecular Engineering Institute, Kinki University,11-6 Kayanomori, Iizuka, Fukuoka 820-8555, Japan.

[1] K. Fujiwara, in *Positron Annihilation, Proceedings of the 6th International Conference on Positron Annihilation, 1982*, edited by P. G. Coleman, S. C. Sharma, and L. M. Diana (North-Holland, Amsterdam, 1982), p. 615.

[2] T. Hyodo, in *Positron Annihilation, Proceedings of the 7th International Conference on Positron Annihilation, 1985*, edited by P. C. Jain, R. M. Singru, and K. P. Gopinathan (World Scientific, Singapore, 1985), p. 643.

[3] A. Dupasquier, in *Positron Solid-State Physics*, edited by W. Brandt and A. Dupasquier (North-Holland, Amsterdam, 1983), p. 510.

[4] O. E. Mogensen, *Positron Annihilation in Chemistry* (Springer, New York, 1995).

[5] H. Saito and T. Hyodo, Phys. Rev. Lett. **90**, 193401 (2003).

[6] Y. Takakusa and T. Hyodo, J. Phys. Soc. Jpn. **49**, 2243 (1980).

[7] T. Hyodo, J. Kasai, and Y. Takakusa, J. Phys. Soc. Jpn. **49**, 2248 (1980).

[8] J. Kasai, T. Hyodo, and K. Fujiwara, J. Phys. Soc. Jpn. **52**, 3671 (1983).

[9] T. Hyodo and A. T. Stewart, Phys. Rev. B **29**, 4164 (1984).

[10] J. Kasai, T. Hyodo, and K. Fujiwara, J. Phys. Soc. Jpn. **57**, 329 (1988).

[11] T. Hyodo, M. Kakimoto, Y. Nagashima, and K. Fujiwara, Phys. Rev. B **40**, 8037 (1989).

[12] I. V. Bondarev and T. Hyodo, Phys. Rev. B **57**, 11 341 (1998).

[13] M. Ueta, H. Kanzaki, K. Kobayashi, Y. Toyozawa, and E. Hanamura, *Excitonic Processes in Solids* (Springer, New York, 1983).

[14] K. S. Song and R. T. Williams, *Self-Trapped Excitons* (Springer, New York, 1993).

[15] K. Nasu and Y. Toyozawa, J. Phys. Soc. Jpn. **50**, 235 (1981).

[16] A. B. Kunz and J. T. Weber, Solid State Commun. **39**, 831 (1981).

[17] R. T. Williams and K. S. Song, J. Phys. Chem. Solids **51**, 679 (1990).

[18] R. Linder, R. T. Williams, and M. Reichling, Phys. Rev. B **63**, 075110 (2001).

[19] M. Kakimoto, T. Hyodo, and K. Fujiwara, in *Positron Annihilation, Proceedings of the 7th International Conference on Positron Annihilation, 1985*, edited by P. C. Jain, R. M. Singru, and K. P. Gopinathan (Ref. 2), p. 776.

[20] I. V. Bondarev, Phys. Rev. B **58**, 12 011 (1998).

[21] A. Sumi and H. Sumi, J. Phys. Soc. Jpn. **54**, 653 (1985).

[22] Y. Toyozawa and A. Sumi, in *Proceedings of the 12th International Conference on Physics of Semiconductors*, edited by B. G. Teubner (Stuttgart, 1974), p. 179.

[23] Y. Nagai, Y. Nagashima, J. Kim, Y. Itoh, and T. Hyodo, Nucl. Instrum. Methods Phys. Res. B **171**, 199 (2000).

[24] Y. Nagashima and T. Hyodo, Phys. Rev. B **41**, 3937 (1990).